

# Specific Shrinkage of Carotid Forks in Moyamoya Disease: A Novel Key Finding for Diagnosis

Satoshi KURODA,<sup>1</sup> Daina KASHIWAZAKI,<sup>1</sup> Naoki AKIOKA,<sup>1</sup> Masaki KOH,<sup>1</sup>  
Emiko HORI,<sup>2</sup> Manabu NISHIKATA,<sup>3</sup> Kimiko UMEMURA,<sup>2</sup> Yukio HORIE,<sup>2</sup>  
Kyo NOGUCHI,<sup>4</sup> and Naoya KUWAYAMA<sup>1</sup>

*Departments of <sup>1</sup>Neurosurgery and <sup>4</sup>Radiology, Graduate School of Medicine and  
Pharmacological Sciences, University of Toyama, Toyama, Toyama;*

*<sup>2</sup>Department of Neurosurgery, Stroke Center, Saiseikai Toyama Hospital, Toyama, Toyama;*

*<sup>3</sup>Department of Neurosurgery, Saiseikai Takaoka Hospital, Takaoka, Toyama*

## Abstract

This study was aimed to analyze the outer diameter of the involved arteries in moyamoya disease, using three-dimensional (3D) constructive interference in steady state (CISS) and direct surgical inspection. Radiological evaluation was performed in 64 patients with moyamoya disease. As the controls, six patients with severe middle cerebral artery (MCA) stenosis and 17 healthy subjects were also recruited. On 3D-CISS, the outer diameter was quantified in the supraclinoid portion of internal carotid artery (C1), the horizontal portions of MCA (M1) and anterior cerebral artery (A1), and basilar artery. The involved carotid fork was directly observed during surgery in another series of three adult patients with moyamoya disease. In 53 adult patients with moyamoya disease, the outer diameters of C1, M1, and A1 segments were  $2.3 \pm 0.7$  mm,  $1.3 \pm 0.5$  mm, and  $1.0 \pm 0.4$  mm in the involved side ( $n = 91$ ), being significantly smaller than the control ( $n = 17$ ), severe M1 stenosis ( $n = 6$ ), and non-involved side in moyamoya disease ( $n = 15$ ,  $P < 0.01$ ). There were significant correlations between Suzuki's angiographical stage and the outer diameters of C1, M1, and A1 ( $P < 0.001$ ). The laterality ratio of C1 and M1 was significantly smaller in unilateral moyamoya disease ( $n = 20$ ) than the controls and severe MCA stenosis ( $P < 0.01$ ). Direct observations revealed a marked decrease in the outer diameter of the carotid fork ( $n = 3$ ). These findings strongly suggest specific shrinkage of the involved arteries in moyamoya disease, which may provide essential information to distinguish moyamoya disease from other intracranial arterial stenosis and shed light on the etiology and novel diagnosis cue of moyamoya disease.

Key words: moyamoya disease, three-dimensional constructive interference in steady state, carotid fork, outer diameter, diagnosis

## Introduction

Moyamoya disease is an uncommon cerebrovascular disorder that is characterized by progressive occlusion of the supraclinoid internal carotid artery (ICA) and its main branches within the circle of Willis. This occlusion results in the dilation of perforating arteries at the base of brain (moyamoya vessels). Histopathological findings in the carotid terminations include fibrocellular thickening of the intima, an irregular undulation (waving) of the internal elastic lamina, and attenuation of the media, all of which have been believed to initiate the luminal stenosis

in moyamoya disease for these four decades.<sup>1–3)</sup> In fact, the diagnosis of moyamoya disease has been based on the radiological information of intraluminal stenosis in the carotid fork.<sup>4)</sup> The concept is quite similar to diagnosis process in atherosclerotic arterial stenosis.

Even now, however, it is not rare to experience the difficulty to distinguish moyamoya disease from intracranial arterial stenosis in a certain population of patients. Furthermore, our recent knowledge on susceptibility gene for moyamoya disease has embossed unclear border between moyamoya disease and intracranial arterial stenosis.<sup>5)</sup> These issues may result from previous diagnostic concept on the basis of radiological information

of intraluminal stenosis. In this study, therefore, the outer diameter of the involved arteries was precisely analyzed on three-dimensional constructive interference in steady state (3D-CISS) images and was also directly inspected during surgery in patients with moyamoya disease.

## Materials and Methods

### I. Patients

In this prospective study, the outer diameter of the intracranial arteries around the circle of Willis was determined in 64 patients with moyamoya disease, using 3D-CISS. All of them were diagnosed as moyamoya disease based on the guideline for the diagnosis of moyamoya disease set by the Research Committee on Moyamoya Disease of the Ministry of Health, Welfare, and Labor of Japan. There were 11 children and 53 adults. There were 27 males and 37 females. Mean age was  $9.8 \pm 4.1$  years and  $44.6 \pm 14.5$  years in pediatric and adult patients, respectively. In pediatric patients, clinical diagnosis included transient ischemic attack (TIA) in seven and ischemic stroke in four. In adult patients, clinical diagnosis included TIA in 22, ischemic stroke in 18, intracranial hemorrhage in 10, and asymptomatic in 3. Of these 64 patients, 44 were defined as bilateral type and other 20 were defined as unilateral type.

To compare with radiological findings in moyamoya disease, this study also included six patients with severe ( $> 80\%$ ) stenosis of the horizontal portion of middle cerebral artery (MCA; M1). There were five males and one female. Mean age was  $62.0 \pm 15.7$  years. Furthermore, this study included totally 17 healthy controls without any history of cerebrovascular disorders. There were 13 males and 4 females. Mean age was  $57.5 \pm 13.3$  years.

In another series of three adult patients with moyamoya disease, the carotid fork was directly observed under surgical microscope during clipping surgery for the aneurysms originated from the internal carotid artery-anterior choroidal artery junction, anterior communicating artery, and basilar artery (BA)-superior cerebellar artery junction.

### II. Radiological examinations

Magnetic resonance (MR) imaging, MR angiography, and cerebral angiography were performed in all 64 patients with moyamoya disease. Disease stage was classified into six stages according to Suzuki's angiographic stage.<sup>3)</sup> MR imaging was performed on a clinical 1.5T or 3T MR imaging unit (Magnetom Avanto or Verio, Siemens AG, Erlangen, Germany) using a standard 12-channel

head coil. T<sub>1</sub>-weighted images, T<sub>2</sub>-weighted images, T<sub>2</sub>\*-weighted images, fluid attenuated inversion recovery (FLAIR) images, and diffusion-weighted images were obtained to locate ischemic and hemorrhagic lesions in the brain parenchyma. In this study, 3D-CISS images were obtained in the evaluation of the outer diameter of the intracranial arteries. Parameters for the 3D-CISS at 1.5T were as follows: repetition time (TR), 9.94 ms; echo time (TE), 4.97 ms; flip angle, 70°; matrix size, 256 × 256; slice thickness, 0.7 mm; field of view (FOV), 160 mm; voxel size, 0.6 × 0.5 × 0.7 mm; number of excitations (NEX), one; scan time, 4 min 16 sec. Parameters for the 3D-CISS at 3T were as follows: TR, 6.59 ms; TE, 2.77 ms; flip angle, 40°; matrix size, 307 × 307; slice thickness, 0.6 mm; FOV, 160 mm; voxel size, 0.5 × 0.4 × 0.6 mm; NEX, one; scan time, 4 min 24 sec.

The outer diameter of involved arteries was measured at the site where the outer diameter was smallest in the involved arteries. As a result, the outer diameter was quantified at the C1 just proximal to the bifurcation and at the M1 and A1 around 3–5 mm distal to the origins in a majority of cases with moyamoya disease.

### III. Statistical analysis

Data were expressed as mean ± standard deviation (SD). Continuous variables were compared among more than three groups, using one-factor analysis of variance (ANOVA) followed by Tukey's post hoc test. Differences were considered statistically significant if the P value was  $< 0.05$ .

## Results

### I. Outer diameter of involved arteries in adult moyamoya disease

Using 3D-CISS, the outer diameter of involved arteries was quantified in patients with moyamoya disease, and was compared with those in the controls and patients with severe M1 stenosis. For this purpose, the data in 11 pediatric patients were excluded, because no control data in healthy children were obtained in this study. As a result, the data in 106 sides of 53 adult patients were analyzed. Of these 106 sides, 91 were involved and other 15 were not involved (stage 0).

Fig. 1 demonstrates representative findings on 3D-CISS in a patient with severe M1 stenosis and that with moyamoya disease. The results are summarized in Table 1. The outer diameter of C1, M1, A1, and BA in the controls was  $3.8 \pm 0.5$  mm,  $3.0 \pm 0.3$  mm,  $2.0 \pm 0.3$  mm, and  $3.4 \pm 0.5$  mm, respectively. There were no significant differences in their outer

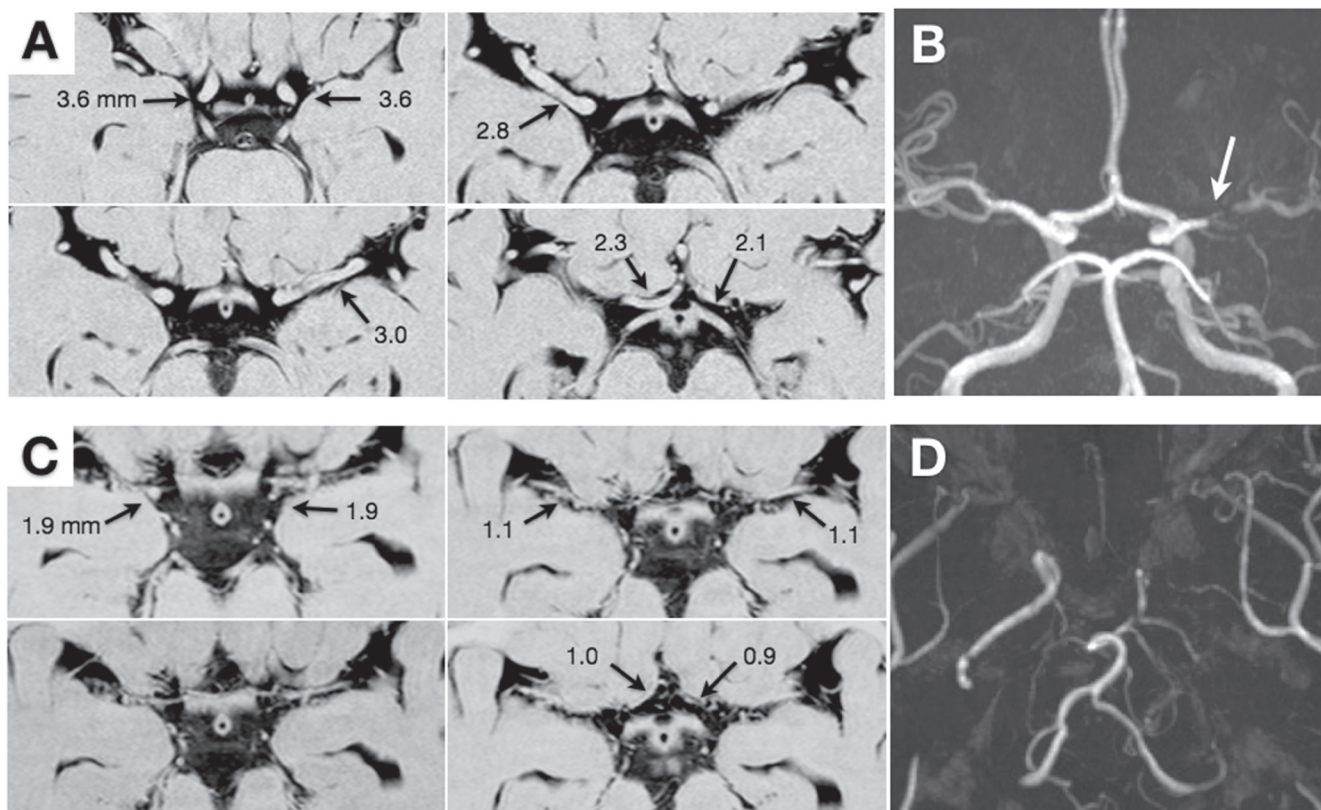


**Fig. 1** Representative three-dimensional constructive interference in steady state (A, C) and magnetic resonance (MR) angiography findings (B, D) of a 41-year-old male with severe stenosis of the left middle cerebral artery (A, B) and a 36-year-old female with bilateral moyamoya disease (C, D). A: The outer diameter of the bilateral C1, M1, and A1 is printed. B: MR angiography shows severe stenosis of the left M1 (arrow). C: The outer diameter of the bilateral C1, M1, and A1 is printed. D: On MR angiography, the internal carotid arteries are occluded on both sides, being graded as stage 5.

**Table 1** Outer diameters of intracranial arteries in normal controls, M1 stenosis, and “adult” moyamoya disease on three-dimensional constructive interference in steady state

	Age (yr)	N	C1 (mm)	M1 (mm)	A1 (mm)	BA (mm)
Control	57.5 ± 13.3	17	3.8 ± 0.5	3.0 ± 0.3	2.0 ± 0.3	3.4 ± 0.5
M1 stenosis						
Ipsilateral	62.0 ± 15.7	6	3.8 ± 0.8	2.7 ± 0.4	1.8 ± 0.2	3.6 ± 0.4
Contralateral		6	3.9 ± 0.4	2.7 ± 0.3	2.1 ± 0.6	3.7 ± 0.4
Moyamoya						
Stage 0	45.4 ± 11.2	15	3.6 ± 0.6	2.7 ± 0.5	1.6 ± 0.5	2.9 ± 0.6
Stage 1–6	44.5 ± 15.1	91	2.3 ± 0.7**	1.3 ± 0.5**	1.0 ± 0.4**	3.1 ± 0.6
Stage 1	49	1	2.7	2.1	1.1	3.2
Stage 2	56.0 ± 10.4	3	2.8 ± 0.3**	2.3 ± 0.4	1.6 ± 0.2	3.3 ± 0.2
Stage 3	34.3 ± 10.5	34	2.4 ± 0.6	1.4 ± 0.4**	1.1 ± 0.4**	2.9 ± 0.6
Stage 4	47.2 ± 14.3	18	2.7 ± 0.7	1.3 ± 0.4	1.0 ± 0.6	3.2 ± 0.6
Stage 5	50.0 ± 13.7	26	1.9 ± 0.5 <sup>§§</sup>	1.1 ± 0.4	0.9 ± 0.3	3.3 ± 0.5
Stage 6	57.7 ± 16.0	9	1.6 ± 0.4	1.2 ± 0.4	0.8 ± 0.3 <sup>###</sup>	3.3 ± 0.6

\*:  $P < 0.05$ , \*\*:  $P < 0.01$  vs. control and stage 0, <sup>§§</sup>:  $P < 0.01$  vs. stage 2, <sup>###</sup>:  $P < 0.01$  vs. stage 3, One-factor analysis of variance (ANOVA) followed by Tukey’s post hoc test, BA: basilar artery.

diameter between the control, severe M1 stenosis, and non-involved side in moyamoya disease. On the other hand, the outer diameter of C1, M1, A1, and BA in the involved sides of moyamoya disease was  $2.3 \pm 0.7$  mm,  $1.3 \pm 0.5$  mm,  $1.0 \pm 0.4$  mm, and  $3.1 \pm 0.6$  mm, respectively. The values of C1, M1, and A1 were significantly smaller in moyamoya disease than the controls and patients with severe M1 stenosis ( $P < 0.01$ ).

Based on Suzuki's angiographical stage, totally 106 sides of 53 adult patients with moyamoya disease were classified into stage 0 in 15 sides, stage 1 in 1, stage 2 in 3, stage 3 in 34, stage 4 in 18, stage 5 in 26, and stage 6 in 9 (Table 1). The outer diameter of C1 was  $2.8 \pm 0.3$  mm in stage 2, being significantly smaller than those in stage 0 and the control ( $P < 0.01$ ). The value was  $1.9 \pm 0.5$  mm in stage 5, being significantly smaller than that in stage 2 ( $P < 0.01$ ). The outer diameter of M1 was  $2.7 \pm 0.5$  mm in stage 0. The value was  $1.4 \pm 0.4$  mm in stage 3, being significantly smaller than those in stage 0 and the control ( $P < 0.01$ ). The outer diameter of A1 was  $1.6 \pm 0.5$  mm in stage 0. The value was  $1.1 \pm 0.4$  mm in stage 3, being significantly smaller than those in stage 0 and the control ( $P < 0.01$ ). The A1 portion had further smaller outer diameter in stage 6 ( $0.8 \pm 0.3$  mm,  $P < 0.01$ ). There were no significant differences in the outer diameter of BA among six stage groups. As shown in Fig. 2, there were significant correlations between Suzuki's angiographical stage and the outer diameters of C1 ( $P < 0.001$ ,  $r^2 = 0.424$ ), M1 ( $P < 0.001$ ,  $r^2 = 0.485$ ), and A1 ( $P < 0.001$ ,  $r^2 = 0.203$ ).

## II. Laterality of involved arteries in unilateral moyamoya disease

As the next step, the ipsilateral-to-contralateral ratio of the outer diameter of involved arteries was calculated in 20 patients with unilateral moyamoya disease, because the intracranial arteries in the non-involved side (stage 0) could be used as the inner references. Both pediatric ( $n = 5$ ) and adult patients ( $n = 15$ ) were included in this analysis, because the ratio may be constant over patients' age. In the controls ( $n = 17$ ), the ratio of C1, M1, and A1 was  $0.99 \pm 0.07$ ,  $0.98 \pm 0.04$ , and  $1.00 \pm 0.14$ , respectively. In patients with severe M1 stenosis ( $n = 6$ ), the ratio of C1, M1, and A1 was  $1.01 \pm 0.09$ ,  $1.06 \pm 0.06$ , and  $0.95 \pm 0.27$ , respectively. The data did not differ between them.

The disease stage in 20 patients with unilateral moyamoya disease was defined as stage 3 in 13 patients, stage 4 in 6, and stage 6 in 1. Fig. 3 demonstrates representative 3D-CISS findings in

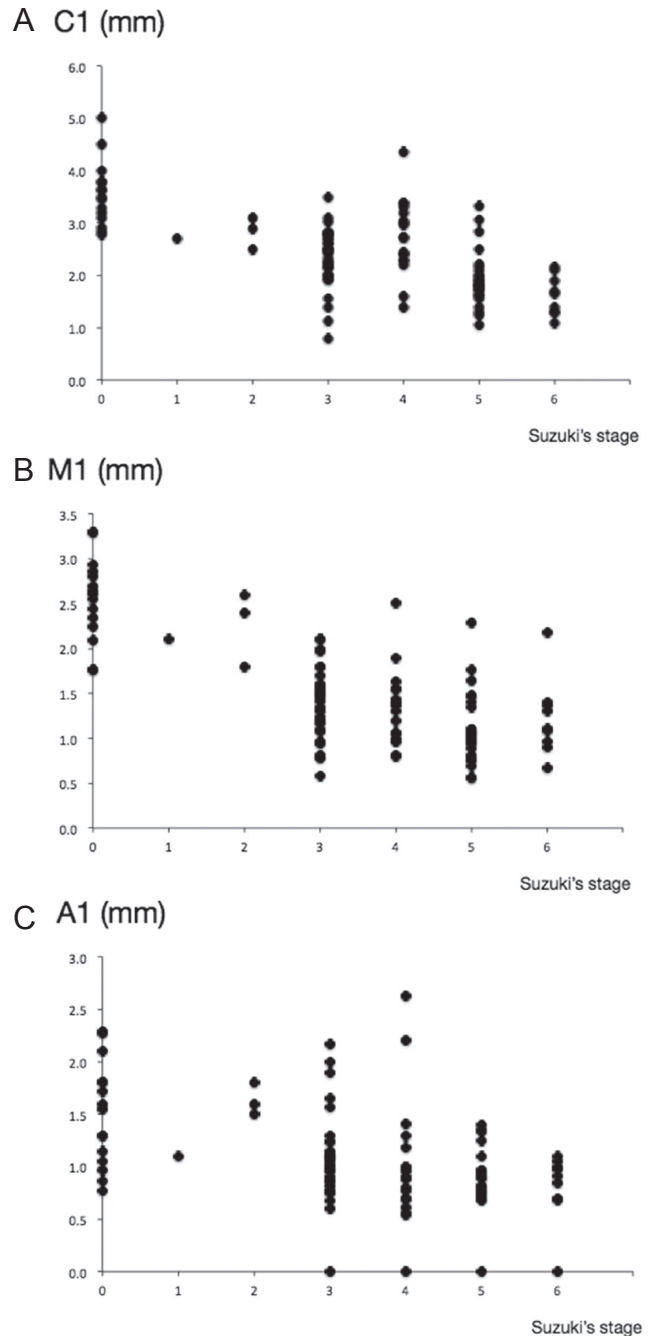


**Fig. 2** Plotted graphs show the relationship between Suzuki's angiographical stage and the outer diameter of the C1 (A), M1 (B), and A1 (C) on three-dimensional constructive interference in steady state, respectively.

unilateral moyamoya disease. In patients with unilateral moyamoya disease, the ratio of C1, M1, and A1 was  $0.68 \pm 0.13$ ,  $0.54 \pm 0.15$ , and  $0.83 \pm 0.34$ , respectively. Therefore, they had significantly lower ratio of C1 and M1 than the controls and patients with severe M1 stenosis ( $P < 0.001$ ; Fig. 4).

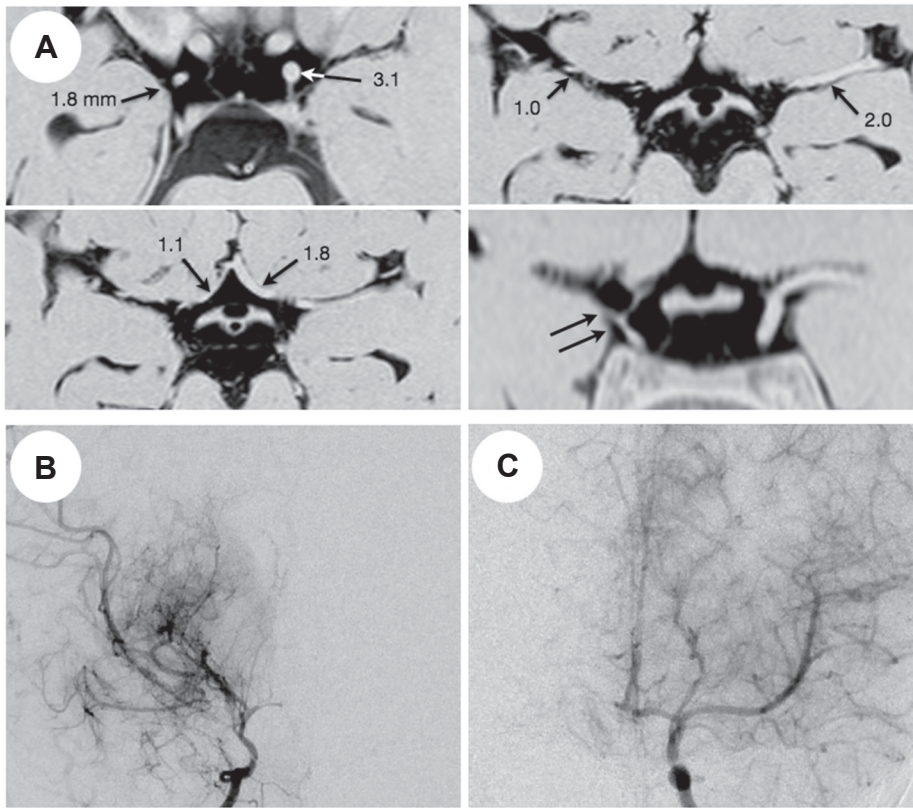


**Fig. 3** Representative three-dimensional constructive interference in steady state (A) and magnetic resonance angiography findings (B, C) of a 4-year-old girl with unilateral moyamoya disease. A: The outer diameter of the bilateral C1, M1, and A1 is printed. Note the marked shrinkage of the right carotid fork on a coronal image (*double arrows*). B: Right carotid angiogram shows severe stenosis of the carotid fork and marked development of basal moyamoya vessels, being graded as stage 3. C: Left carotid angiogram shows no definite abnormality (stage 0).

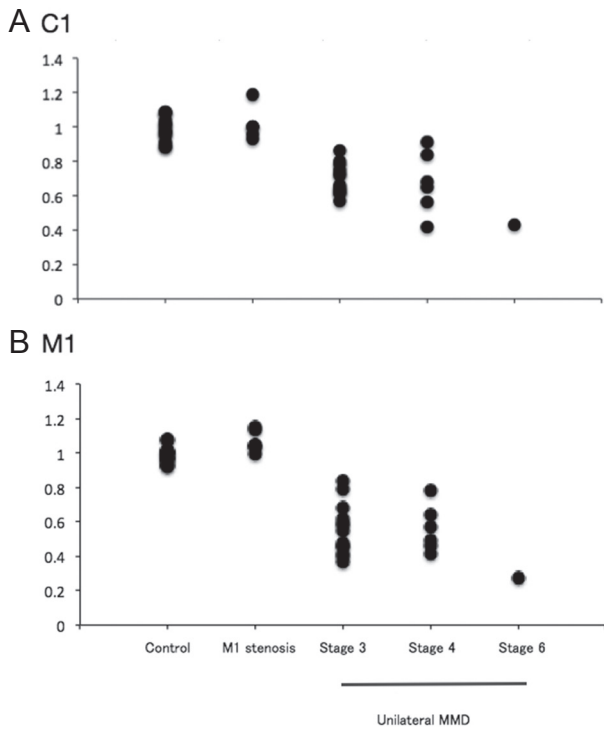


**Fig. 4** Plotted graphs show the ipsilateral to contralateral ratio of the outer diameter of the C1 (A) and M1 (B) in normal controls, severe M1 stenosis, and unilateral moyamoya disease. In unilateral moyamoya disease, the data are shown according to Suzuki's angiographical stage.

### III. Direct observation of carotid fork in adult moyamoya disease

The carotid fork was directly observed during surgery in three adult patients (Fig. 5). Two of them were male and another was female. Their age was 48 years, 65 years, and 29 years, respectively. In all three patients, the C1, proximal M1, and A1 segments were white-colored, and their outer diameter was much smaller than usual on visual inspection. However, the distal portion of M1 segment had normal red color and larger outer diameter than its proximal portion (Fig. 5). The outer diameter of the C1, proximal M1, and A1 segments was semi-quantitatively determined as the ratio to that of the anterior choroidal artery in each case. As a result, the ratio in the C1, M1, and A1 segment was  $1.50 \pm 0.25$ ,  $1.13 \pm 0.38$ , and  $0.87 \pm 0.29$ , respectively. According to Lang (2001), the intracranial ICA and anterior choroidal artery had an average diameter of 3.26 (2.2–4.3) mm and 0.77 (0.4–1.25) mm, respectively.<sup>6)</sup> Therefore, the diameter ratio of ICA to anterior choroidal artery can be calculated as 4.23. As a result, the mean value of 1.50 in our series would be much lower than normal controls. Likewise, the average diameter of M1 and A1 segments is 2.7 mm and 2.1 mm in the normal subjects.<sup>6)</sup> Their diameter ratio to anterior choroidal artery can be calculated as 3.51 and

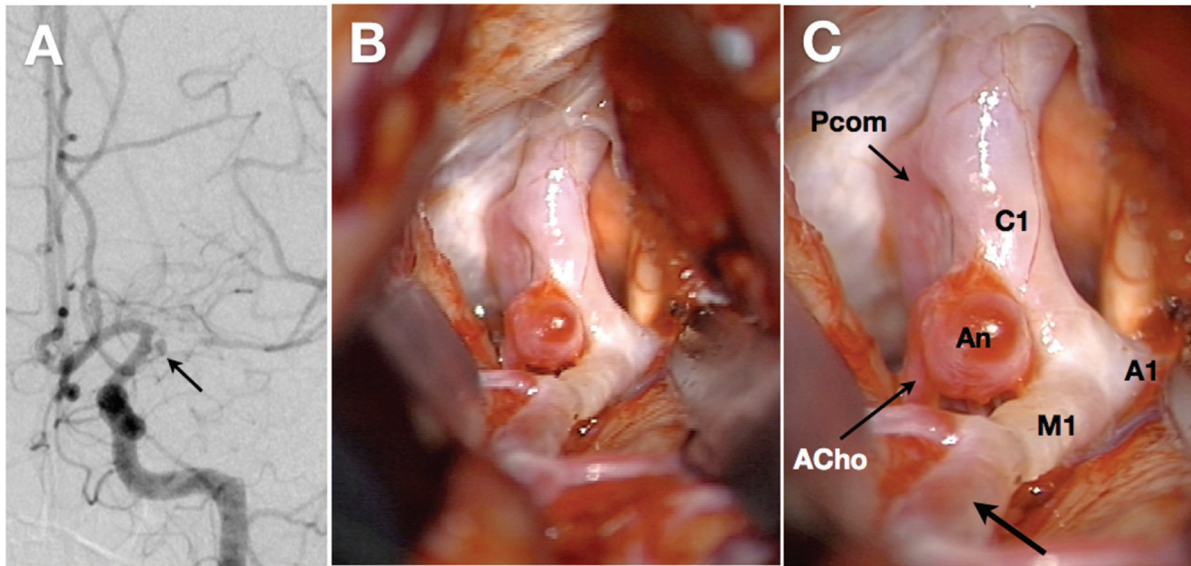


**Fig. 5** Radiological and intraoperative findings of a 29-year-old female with moyamoya disease. **A:** Left carotid angiography reveals a stenosis in the left carotid fork and dilated moyamoya vessels. The horizontal portion of the left middle cerebral artery is severely stenotic. Note the saccular aneurysm (An) arising from the internal carotid artery-anterior choroidal artery junction (*arrow*). **B, C:** Direct inspection during surgery reveals that the left supraclinoid portion of internal carotid artery (C1) is severely constricted and white-colored, compared with the posterior communicating artery (Pcom) and anterior choroidal artery (ACho). The horizontal portions of middle (M1) and anterior cerebral arteries (A1) look very similar. Note that the distal segment of M1 has the normal red-colored appearance (**C, arrow**).

2.73, being much higher than 1.13 and 0.87 in our series, respectively.

## Discussion

Based on radiological and surgical observations, this study clearly shows that the involved arteries decrease their outer diameter in both bilateral and unilateral moyamoya disease. When disease stage progresses, they further decrease their outer diameter in bilateral moyamoya disease. In unilateral moyamoya disease, however, the ratio of the ipsi- to contralateral side did not differ among the disease stage probably because of limited number of samples. The findings are pathognomonic in moyamoya disease. Direct surgical observations support these radiological findings. Previously, there were several studies to evaluate the outer diameter of the involved arteries in moyamoya disease. Using 3D-CISS, Kaku et al. (2012) reported that the outer diameter of ICA and M1 segment is significantly smaller in moyamoya disease than in the control and in M1 stenosis or occlusion. However, they did not evaluate the relationship between their outer diameters and Suzuki's angiographical stage. Their study also included a significant number of pediatric patients when measuring the outer diameter on 3D-CISS, which

may underestimate the values in moyamoya disease because the vessel size is smaller in children than in adults.<sup>7)</sup> Kim et al. (2013) compared the outer diameter of M1 in 12 patients with moyamoya disease and 20 patients with intracranial atherosclerotic disease, and reported that the outer diameter was significantly smaller in the former than in the latter.<sup>8)</sup> Ryoo et al. (2014) also found the shrinkage of M1 segment in 23 patients with moyamoya disease, but concluded that the outer diameter did not differ between stage 1–3 and stage 4–6.<sup>9)</sup> Therefore, this is the first study that precisely analyzes the relationship between disease stage and the outer diameter of the involved arteries in a significant number of adult patients with moyamoya disease.

Furthermore, this is the first report to support the 3D-CISS findings by directly observing the carotid fork during surgery in adult patients with moyamoya disease. Surprisingly, the C1, proximal M1, and A1 segments were markedly constricted and white-colored, confirming our preliminary findings.<sup>2)</sup> The diameter ratio of these segments to anterior choroidal artery was clearly smaller in moyamoya disease than in the normal subjects.<sup>6)</sup> The finding is extremely notable, even thinking about the fact that the anterior choroidal artery is abnormally dilated to supply collateral blood flow in moyamoya

disease. Therefore, the carotid fork is considered abnormally constricted in moyamoya disease. Sample size in this study ( $n = 3$ ) may be quite small, but it would continue to remain difficult to survey it in larger cohort, because it is quite rare to directly operate on the intracranial aneurysms associated with moyamoya disease nowadays.

Only few histopathological studies have previously paid attention to their outer diameter in moyamoya disease.<sup>10,11</sup> As aforementioned, histopathological findings in the involved arteries include fibrocellular thickening of the intima, an irregular undulation (waving) of the internal elastic lamina, and attenuation of the media, which are very specific for moyamoya disease. As with atherosclerosis, intimal thickening may contribute to luminal stenosis. Recent study has suggested that the circulating endothelial progenitor cells may contribute to intimal thickening in moyamoya disease.<sup>12</sup> On the other hand, attenuation of the media may induce the decrease in arterial wall volume and be related to the narrowing of their outer diameter in moyamoya disease. Takagi et al. (2006) found caspase-3-induced apoptosis in the media of MCA

obtained from patients with moyamoya disease.<sup>13</sup> However, few studies have previously discussed the pathophysiological significance of irregular waving of the internal elastic lamina in moyamoya disease. Considering the shrinkage of involved arteries, this unusual phenomenon may be one of important manifestations to decode the unsolved etiology in moyamoya disease. Very interestingly, Uchida et al. (2011) produced a model of coronary artery spasm in the beagles and found that the internal elastic lamina are markedly folded like the “bellows of an old-fashioned camera,” suggesting that this phenomenon may play an essential role in coronary artery spasm which causes the narrowing of outer diameter.<sup>14</sup> Histological findings in coronary spasm are very similar to those in moyamoya disease. Taken together, we tentatively propose the hypothesis that both luminal stenosis and outer diameter narrowing may simultaneously develop in the carotid forks and initiate moyamoya disease. Folding of the elastic lamina may play a key role in the outer diameter narrowing through the mechanisms similar to spasm (Fig. 6). The scheme is quite different from the phenomenon of “positive” remodeling that can be

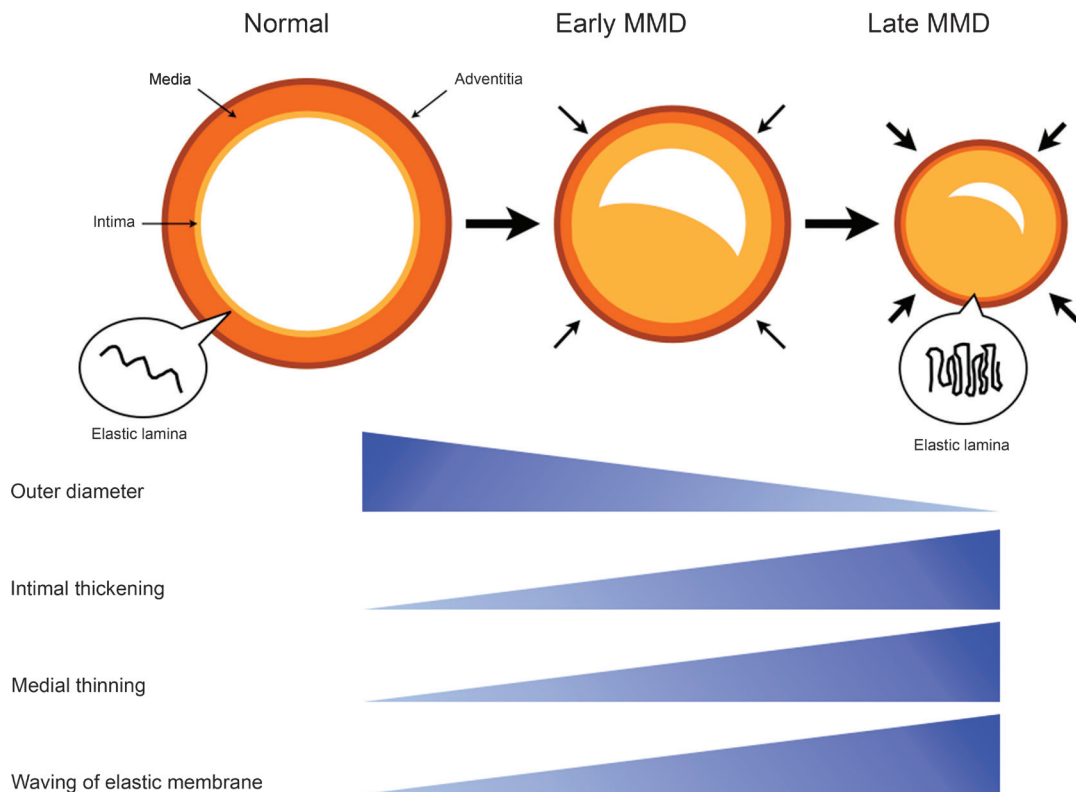


**Fig. 6** The diagram shows a novel hypothesis of moyamoya disease development. As pointed out previously, the intimal thickening causes luminal stenosis in the carotid fork. At the same time, however, the carotid fork starts to decrease the outer diameter. These changes gradually progress the disease stage. Both the medial thinning and the waving of elastic lamina may be closely related to the shrinkage of carotid fork. MMD: moyamoya disease.

observed in atherosclerosis.<sup>15)</sup> Future studies should be planned to explore the underlying mechanisms of moyamoya disease from this viewpoint.

Recently, there are some preliminary trials to treat the occlusive lesion in moyamoya disease, using endovascular technique.<sup>16–21)</sup> However, a significant number of patients require repeat treatment because of restenosis, and some of them suffer severe intracranial bleeding.<sup>19,20)</sup> The present results strongly suggest that endovascular treatments to directly dilate the stenotic lumen in the carotid forks may be ineffective or sometimes dangerous, because the involved arteries have the decreased outer diameter.

For these four decades, the diagnosis of moyamoya disease has been based on radiological findings including stenosis or occlusion of the terminal portion of the internal carotid artery and its main branches. Namely, the diagnosis completely depends on the information within the lumen in the involved arteries.<sup>4)</sup> Even now, therefore, it is sometimes difficult to distinguish the patients with moyamoya disease from those with atherosclerotic intracranial arterial stenosis.<sup>8,22)</sup> Based on these observations, we would like to propose careful considerations to revise the diagnosis criteria of moyamoya disease by adding the findings on 3D-CISS to conventional criteria in near future. Such refinement of diagnosis criteria would make us to identify the patients with moyamoya disease more easily and sensitively. Furthermore, recent study has also indicated that a certain subgroup of patients with intracranial major artery stenosis/occlusion has a common genetic variant, ring finger 213 (RN213) c.14576G>A, known as a susceptibility gene for moyamoya disease.<sup>5)</sup> Precise 3D-CISS examinations may also be useful to evaluate the impacts of genetic variant on the subtypes of intracranial major artery stenosis/occlusion, including moyamoya disease.

In conclusion, this study clearly demonstrates specific shrinkage of the involved arteries in moyamoya disease. As the disease stage progresses, their outer diameter decreases. The findings are quite different from those in atherosclerotic intracranial arterial stenosis. Their “specific” shrinkage may provide novel diagnostic information to distinguish moyamoya disease from other intracranial arterial stenosis and shed light on the etiology of moyamoya disease.

### Acknowledgments

The authors deeply thank Dr. Hitoshi Matsuzawa, Department of Integrated Neuroscience, Brain Research Institute Center for Integrated Human Brain Science, Niigata University, Niigata, Japan, for his critical comments on the present results. This study was supported by a grant from the Research Committee

on Moyamoya Disease, sponsored by the Ministry of Health, Labor, and Welfare of Japan.

### Conflicts of Interest Disclosure

None.

### References

- 1) Fukui M: Current state of study on moyamoya disease in Japan. *Surg Neurol* 47: 138–143, 1997
- 2) Kuroda S, Houkin K: Moyamoya disease: current concepts and future perspectives. *Lancet Neurol* 7: 1056–1066, 2008
- 3) Suzuki J, Takaku A: Cerebrovascular “moyamoya” disease. Disease showing abnormal net-like vessels in base of brain. *Arch Neurol* 20: 288–299, 1969
- 4) Research Committee on the Pathology and Treatment of Spontaneous Occlusion of the Circle of Willis; Health Labour Sciences Research Grant for Research on Measures for Intractable Diseases: Guidelines for diagnosis and treatment of moyamoya disease (spontaneous occlusion of the circle of Willis). *Neurol Med Chir (Tokyo)* 52: 245–266, 2012
- 5) Miyawaki S, Imai H, Shimizu M, Yagi S, Ono H, Mukasa A, Nakatomi H, Shimizu T, Saito N: Genetic variant RNF213 c.14576G>A in various phenotypes of intracranial major artery stenosis/occlusion. *Stroke* 44: 2894–2897, 2013
- 6) Lang J: Cerebral arterial circle in adults and aneurysms, in Lang J (ed): *Skull Base and Related Structures, ed 2*. Stuttgart, Schattauer, 2001, pp 31–48
- 7) Kaku Y, Morioka M, Ohmori Y, Kawano T, Kai Y, Fukuoka H, Hirai T, Yamashita Y, Kuratsu J: Outer-diameter narrowing of the internal carotid and middle cerebral arteries in moyamoya disease detected on 3D constructive interference in steady-state MR image: is arterial constrictive remodeling a major pathogenesis? *Acta Neurochir (Wien)* 154: 2151–2157, 2012
- 8) Kim YJ, Lee DH, Kwon JY, Kang DW, Suh DC, Kim JS, Kwon SU: High resolution MRI difference between moyamoya disease and intracranial atherosclerosis. *Eur J Neurol* 20: 1311–1318, 2013
- 9) Ryoo S, Cha J, Kim SJ, Choi JW, Ki CS, Kim KH, Jeon P, Kim JS, Hong SC, Bang OY: High-resolution magnetic resonance wall imaging findings of Moyamoya disease. *Stroke* 45: 2457–2460, 2014
- 10) Haltia M, Iivanainen M, Majuri H, Puranen M: Spontaneous occlusion of the circle of Willis (moyamoya syndrome). *Clin Neuropathol* 1: 11–22, 1982
- 11) Coakham HM, Duchon LW, Scaravilli F: Moya-moya disease: clinical and pathological report of a case with associated myopathy. *J Neurol Neurosurg Psychiatr* 42: 289–297, 1979
- 12) Sugiyama T, Kuroda S, Nakayama N, Tanaka S, Houkin K: Bone marrow-derived endothelial progenitor cells participate in the initiation of moyamoya disease. *Neurol Med Chir (Tokyo)* 51: 767–773, 2011



- 13) Takagi Y, Kikuta K, Sadamasa N, Nozaki K, Hashimoto N: Caspase-3-dependent apoptosis in middle cerebral arteries in patients with moyamoya disease. *Neurosurgery* 59: 894–900; discussion 900–901, 2006
- 14) Uchida Y, Uchida Y, Matsuyama A, Koga A, Maezawa Y, Maezawa Y, Hiruta N: Functional medial thickening and folding of the internal elastic lamina in coronary spasm. *Am J Physiol Heart Circ Physiol* 300: H423–H430, 2011
- 15) Dolan JM, Kolega J, Meng H: High wall shear stress and spatial gradients in vascular pathology: a review. *Ann Biomed Eng* 41: 1411–1427, 2013
- 16) Rodriguez GJ, Kirmani JF, Ezzeddine MA, Qureshi AI: Primary percutaneous transluminal angioplasty for early moyamoya disease. *J Neuroimaging* 17: 48–53, 2007
- 17) Drazin D, Calayag M, Gifford E, Dalfino J, Yamamoto J, Boulos AS: Endovascular treatment for moyamoya disease in a Caucasian twin with angioplasty and Wingspan stent. *Clin Neurol Neurosurg* 111: 913–917, 2009
- 18) Kim T, Kwon OK, Oh CW, Bang JS, Hwang G, Lee YJ: Intracranial stenting using a drug-eluting stent for moyamoya disease involving supraclinoid ICA: a case report. *Neurol Med Chir (Tokyo)* 54: 136–138, 2014
- 19) Khan N, Dodd R, Marks MP, Bell-Stephens T, Vavao J, Steinberg GK: Failure of primary percutaneous angioplasty and stenting in the prevention of ischemia in Moyamoya angiopathy. *Cerebrovasc Dis* 31: 147–153, 2011
- 20) Eicker S, Etminan N, Turowski B, Steiger HJ, Hänggi D: Intracranial carotid artery stent placement causes delayed severe intracranial hemorrhage in a patient with moyamoya disease. *J Neurointerv Surg* 3: 160–162, 2011
- 21) Santirso D, Oliva P, González M, Murias E, Vega P, Gil A, Calleja S: Intracranial stent placement in a patient with moyamoya disease. *J Neurol* 259: 170–171, 2012
- 22) Wei YC, Liu CH, Chang TY, Chin SC, Chang CH, Huang KL, Chang YJ, Peng TI, Lee TH: Coexisting diseases of moyamoya vasculopathy. *J Stroke Cerebrovasc Dis* 23: 1344–1350, 2014

---

*Address reprint requests to:* Satoshi Kuroda, MD, PhD, Department of Neurosurgery, Graduate School of Medicine and Pharmacological Science, University of Toyama, 2630 Sugitani, Toyama, Toyama 930-0194, Japan.  
*e-mail:* skuroda@med.u-toyama.ac.jp